The lognormal-like statistics of a stochastic squeeze process

Dekel Shapira, Doron Cohen
Department of Physics, Ben-Gurion University of the Negev, Beer-Sheva 84105, Israel

We analyze the full statistics of a stochastic squeeze process. The model's two parameters are the bare stretching rate w, and the angular diffusion coefficient D. We carry out an exact analysis to determine the drift and the diffusion coefficient of $\log(r)$, where r is the radial coordinate. The results go beyond the heuristic lognormal description that is implied by the central limit theorem. Contrary to the common "Quantum Zeno" approximation, the radial diffusion is not simply $D_r = (1/8)w^2/D$, but has a non-monotonic dependence on w/D. Furthermore, the calculation of the radial moments is dominated by the far non-Gaussian tails of the $\log(r)$ distribution.

I. INTRODUCTION

In this paper we analyze the full statistics of a stochastic squeeze process that is described by the Langevin equation (Stratonovich interpretation):

$$\begin{aligned}\dot{x} &= wx - \omega(t)y \\ \dot{y} &= -wy + \omega(t)x\end{aligned} \tag{1}$$

where the average rotation frequency is $\langle\omega(t)\rangle = 0$, with fluctuations that looks like white noise:

$$\langle\omega(t')\omega(t'')\rangle = 2D\delta(t'-t'') \tag{2}$$

Accordingly the model has two parameters: the angular diffusion coefficient D of the polar *phase*, and the bare stretching rate w of the radial coordinate $r = \sqrt{x^2+y^2}$.

The squeeze operation is of interest in numerous fields of science and engineering, but our main motivation originates from the quantum mechanical arena, where it is known as parametric amplification. In particular it describes the dynamics of a Bosonic Josephson junction, given that all the particles are initially condensed in the upper orbital (see [1] and references therein). Such preparation is unstable, but it can be stabilized by introducing frequent measurements or by introducing noise. This is the so-called "quantum Zeno effect" (QZE) [2–6].

The stochastic squeeze process that is described by Eq.(1) constitutes a prototype model for QZE. The model has been considered in [7, 8], and later the shortcomings of its analysis were recognized in [9]. The (x, y) of Eq.(1) are local canonical conjugate coordinates in the vicinity of an hyperbolic (unstable) fixed-point in phase space. The essence of the QZE in this context is the observation that the introduction of the noise leads to slow-down of the quantum decoherence process, meaning that the decay of the initial preparation is suppressed. Namely, for strong noise (large D in Eq.(2)) the radial spreading due to w is inhibited.

Outline.– The QZE motivation for the analysis of Eq.(1) is introduced in Sections II. Numerical results for the radial spreading are presented in Section III. These do not agree with the common expectations and hence motivate the analysis of the phase randomization in Sections IV and V. Consequently the exact calculation of the $\log(r)$ diffusion is presented in Sections VI and VII, while the r moments are analyzed in Sections VIII and IX. Some extra details regarding the QZE perspective and other technicalities are provided in the Appendices.

II. SEMICLASSICAL PERSPECTIVE

In this section we clarify the semiclassical perspective for the QZE model of [7, 8]. Following [9] we motivate the detailed analysis of this model.

For a particular realization of $\omega(t)$ the evolution that is generated by Eq.(1) is represented by a symplectic matrix

$$\begin{pmatrix} x(t) \\ y(t) \end{pmatrix} = \boldsymbol{U} \begin{pmatrix} x_0 \\ y_0 \end{pmatrix} \tag{3}$$

The matrix is characterized by its trace $a = \mathrm{trace}(\boldsymbol{U})$. If $|a| < 2$ it means elliptic matrix (rotation). If $|a| > 2$ it means hyperbolic matrix. In the latter case, the radial coordinate r is stretched in one major direction by some factor $\exp(\alpha)$, while in the other major direction it is squeezed by factor $\exp(-\alpha)$. Hence $a = \pm 2\cosh(\alpha)$. If we operate with $\boldsymbol{U}$ on an initial isotropic cloud that has radius r_0, then we get a stretched cloud with $\langle r^2\rangle = \mathcal{A}\, r_0^2$, where $\mathcal{A} = \cosh(2\alpha)$. For more details see Appendix A. The numerical procedure of generating a stochastic process that is described by Eq. (1) is explained in Appendix B. Rarely the result is a rotation. So from now on we refer to it as "squeeze".

The initial preparation can be formally described as a minimal wavepacket at the origin of phase-space. The local canonical coordinates are (x, y), or optionally one can use the polar coordinates (φ, r). The initial spread of the wavepacket is $\langle r^2\rangle = \hbar$. In the case of a Bosonic Josephson Junction the dimensionless Planck constant is related to the number of particles, namely $\hbar = 2/N$. In the absence of noise ($D = 0$) the wavepacket is stretched exponentially in the x direction, which implies a very fast decay of the initial preparation. This decay can be described by functions $\mathcal{P}(t)$ and $\mathcal{F}(t)$ that give the survival probability of the initial state, and the one-body coherence of the evolving state. For precise definitions see Appendix C.

We now consider the implication of having a noisy dephasing term ($D > 0$). The common perspective is to say

that this noise acts like a measurement of the r coordinate, which randomizes the phase φ over a time scale $\tau \sim 1/D$, hence introducing a "collapse" of the wavefunction. The succession of such interventions (see Appendix C) leads to a relatively slow exponential decay of the coherence, namely $\mathcal{F}(t) = \exp\{-(\hbar/2)\mathcal{S}(t)\}$, where

$$\mathcal{S}(t) \;=\; \left(\frac{w^2}{D}\right) t \tag{4}$$

The stronger the noise (D), the slower is the decay of $\mathcal{F}(t)$. Similar observation applies to $\mathcal{P}(t)$. Using a semiclassical perspective [9] it has been realized that $\mathcal{S}(t) = \mathcal{A}(t) - \mathcal{A}(0)$. Note that by definition $\hbar\mathcal{A}(t)$ is the spread $\langle r^2 \rangle$ of the evolving phase-space distribution.

The well known QZE expression Eq.(4), in spite of its popularity, poorly describes the decoherence process [9]. In fact, it agrees with numerical simulations only for extremely short times for which $(w^2/D)t \ll 1$. The semiclassical explanation is as follows: In each τ-step of the evolution the phase-space distribution is stretched by a random factor $\lambda_n = \exp[\alpha_n]$, where the α_n are uncorrelated random variables. Hence by the central limit theorem the product $\lambda = \lambda_t ... \lambda_2 \lambda_1$ has lognormal distribution, where $\log(\lambda)$ has some average $\mu \propto t$ and variance $\sigma^2 \propto t$ that determine an $\mathcal{A}(t)$ and hence $\mathcal{S}(t)$ that differs from the naive expression of Eq.(4). The essence of the QZE is that μ and σ^2 are inversely proportional to the intensity of the erratic driving. Consequently one has to distinguish between 3 time scales: the "classical" time for phase ergodization $\tau \sim D^{-1}$ which is related to the angular diffusion; the "classical" time for loss of isotropy $t_r \sim (w^2/D)^{-1}$ that characterizes the radial spreading; and the "quantum" coherence time $t_c \sim (1/\hbar)t_r$, after which $\mathcal{F}(t) \ll 1$.

In [9] the time dependence of μ and σ has been determined numerically. Here we would like to work out a proper analytical theory. It turns out that a quantitative analysis of the stochastic squeezing process requires to go beyond the above heuristic description. The complication arises because what we have is not multiplication of random number, but multiplication of random matrices. Furthermore we shall see that the calculation of moments requires to go beyond central limit theorem, because they are dominated by the far tails of the distribution.

In the concluding section X we shall clarify that from an experimental point of view the formal expression $\mathcal{F}(t) = \exp\{-(\hbar/2)\mathcal{S}(t)\}$ is not very useful. For practical purpose it is better to consider the *full* statistics of the Bloch-vector, and to determine μ and σ via a standard fitting procedure.

III. PRELIMINARY CONSIDERATIONS

Below we are not using a matrix language, but address directly the statistical properties of an evolving distribution. In (φ, r) polar coordinates Eq.(1) takes the form

$$\dot{\varphi} \;=\; -w\sin(2\varphi) \;+\; \omega(t) \tag{5}$$
$$\dot{r} \;=\; [w\cos(2\varphi)]\; r \tag{6}$$

We see the equation for the phase decouples, while for the radius

$$\frac{d}{dt}\ln(r(t)) \;=\; w\cos(2\varphi) \tag{7}$$

The RHS has some finite correlation time $\tau \sim 1/D$, and therefore $\ln(r)$ is like a sum of t/τ uncorrelated random variables. It follows from the central limit theorem that for long time the main body of the $\ln(r)$ distribution can be approximated by a *normal* distribution, with some average $\mu \propto t$, and some variance $\sigma^2 \propto t$. Consequently we can define a radial stretching rate w_r and a radial diffusion coefficient D_r via the following asymptotic time

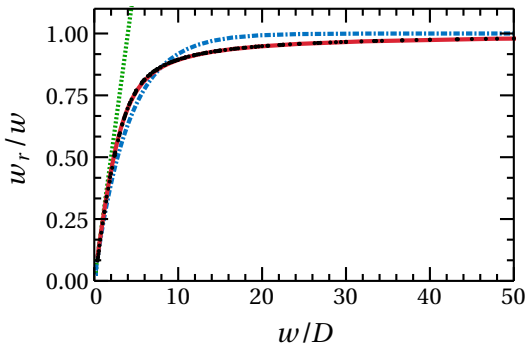

FIG. 1. Scaled stretching rate w_r/w versus w/D. The numerical results (black symbols) are based on simulations with 2000 realizations. The lines are for the naive result Eq.(10) (green dotted); the exact result Eq.(20) (red solid); and its practical approximation Eq.(21) (blue dashed-dotted). For large values of w/D we get $w_r/w = 1$, as for a pure stretch.

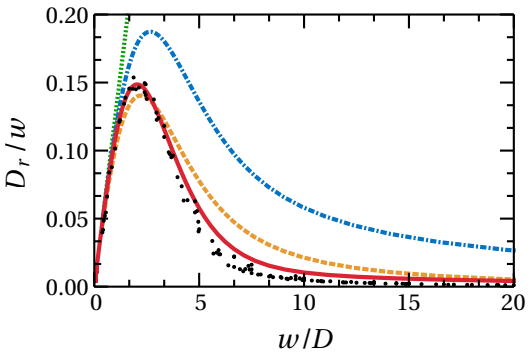

FIG. 2. Scaled diffusion coefficient D_r/w versus w/D. The numerical results (black symbols) are based on simulations with 2000 realizations. The lines are for the naive result Eq.(11) (green dotted); the exact result Eq.(30) (red solid); and the approximation Eq.(25) with $\tau = 1/(2D)$ (blue dashed-dotted), and with Eq.(31) (dashed orange line).

dependence:

$$\mu = w_r t \quad (8)$$
$$\sigma^2 = 2D_r t \quad (9)$$

Our objective is to find explicit expression for w_r and D_r, and also to characterize the full statistics of $r(t)$ in terms of these two parameters, that are determined by the bare model parameters (w, D). We shall see that the statistics of $r(t)$ is described by a *bounded lognormal distribution*.

Some rough estimates are in order. For large D one naively assumes that due to ergodization of the phase $\mu = \langle \cos(2\varphi) \rangle w$ is zero, while $\sigma^2 \sim (w\tau)^2(t/\tau)$. Hence one deduces that $w_r \to 0$ while $D_r \propto w^2/D$. A more careful approach that takes into account the non-isotropic distribution of the phase gives [9] the asymptotic results

$$w_r \sim \frac{w^2}{4D} \quad (10)$$
$$D_r \sim \frac{w^2}{8D} \quad (11)$$

The dimensionless parameter that controls the accuracy of this result is w/D. These approximations are satisfactory for $w/D \ll 1$, and fails otherwise, see Fig.1 and Fig.2. For large w/D we get $w_r \to w$, while $D_r \to 0$.

IV. PHASE ERGODIZATION

The Fokker-Planck equation that is associated with Eq.(5) is

$$\frac{\partial \rho}{\partial t} = \frac{\partial}{\partial \varphi}\left[\left(D\frac{\partial}{\partial \varphi} + w\sin(2\varphi)\right)\rho\right] \quad (12)$$

It has the canonical steady state solution

$$\rho_\infty(\varphi) \propto \exp\left[\frac{w}{2D}\cos(2\varphi)\right] \quad (13)$$

If we neglect the cosine potential in Eq. (12) then the time for ergodization is $\tau_{\rm erg} \sim 1/D$. But if w/D is large we have to incorporate an activation factor, accordingly

$$\tau_{\rm erg} = \frac{1}{D}\exp\left[\frac{w}{D}\right] \quad (14)$$

Fig.3(a) shows the distribution of the phase for two different initial conditions, as obtained by a finite time numerical simulation. It is compared with the steady state solution. The dynamics of r depends only on 2φ, and is dominated by the distribution at the vicinity of $\cos(2\varphi) \sim 1$. We therefore display in Fig. 3(b) the distribution of φ modulo π. We deduce that the transient time of the $\ln(r)$ spreading is much shorter than $\tau_{\rm erg}$.

For the later calculation of w_r we have to know the moments of the angular distribution. From Eq.(13) we obtain:

$$X_n \equiv \langle \cos(2n\varphi) \rangle_\infty = \frac{I_n\left(\frac{w}{2D}\right)}{I_0\left(\frac{w}{2D}\right)} \quad (15)$$

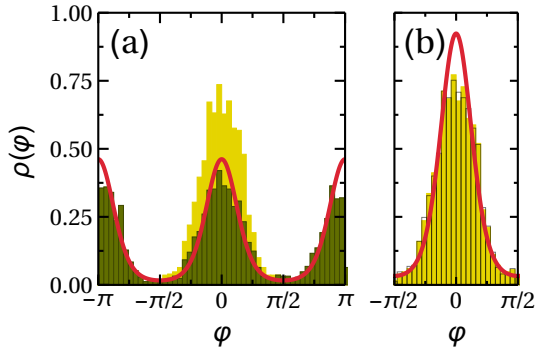

FIG. 3. **(a)** Phase distribution for $(w/D) = 10/3$ after time $(wt) = 6$, with initial conditions $\varphi = 0$ (filled, yellow) and $\varphi = \pi/2$ (green bars) with 2000 realizations. For larger times, both reach the steady state of Eq.(13) (red line). **(b)** The distributions of φ modulo π.

Here $I_n(z)$ are the modified Bessel functions. For small z we have $I_n(z) \approx [1/n!](z/2)^n$, while for large z we have $I_n(z) \approx (2\pi z)^{-1/2}e^z$. The dependence of the X_n on n for representative values of w/D is illustrated in the upper panel of Fig.4.

For the later calculation of D_r we have to know also the temporal correlations. We define

$$C_n(t) = \langle \cos(2n\varphi_t)\cos(2\varphi) \rangle_\infty - X_n X_1 \quad (16)$$

where a constant is subtracted such that $C_n(\infty) = 0$. We use the notations

$$c_n \equiv \int_0^\infty C_n(t)dt \quad (17)$$

and

$$\Delta_n \equiv C_n(0) = \frac{1}{2}(X_{n+1} + X_{n-1}) - X_n X_1 \quad (18)$$

In order to find an asymptotic expression we use

$$I_n(z) \approx \frac{e^z}{\sqrt{2\pi z}}\left[1 - \frac{4n^2-1}{(8z)} + \frac{(4n^2-1)(4n^2-9)}{2(8z)^2}\right]$$

and get

$$\Delta_n \approx 2\left(\frac{w}{D}\right)^{-2} n^2 \quad \text{for} \quad \left(\frac{w}{D}\right) \gg 1 \quad (19)$$

The dependence of the Δ_n on n for representative values of w/D is illustrated in the lower panel of Fig.4.

V. RADIAL SPREADING

If follows from Eq.(7) that the radial stretching rate is

$$w_r = w\langle \cos(2\varphi) \rangle_\infty = X_1 w \quad (20)$$

A rough interpolation for X_1 that is based on the asymptotic expressions for the Bessel functions in Eq.(15) leads to the following approximation

$$w_r \approx w\left[1 - \exp\left(-\frac{w}{4D}\right)\right] \quad (21)$$

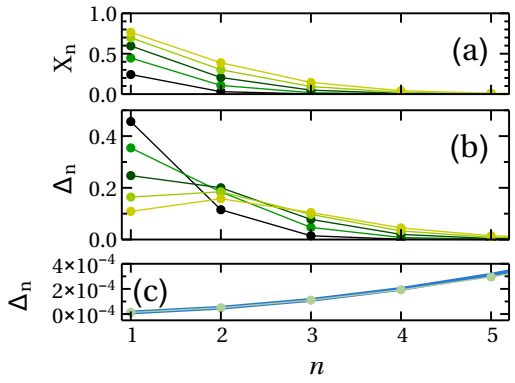

FIG. 4. **(a)** The values of X_n versus n for some values of w/D. From bottom to top $w/D = 1, 2, 3, 4, 5$. **(b)** The values of Δ_n versus n for the same values of w/D, from top to bottom at n=1. **(c)** Δ_n versus n for large w/D. Here $w/D = 400$. The asymptotic approximation Eq.(19) is indicated by blue line.

The exact result as well as the approximation are illustrated in Fig.1 and compared with the results of numerical simulations.

For the second moment it follows from Eq.(7) that the radial diffusion coefficient is

$$D_r \;=\; w^2 \int_0^\infty C_1(t)dt \;=\; c_1 w^2 \qquad (22)$$

If we assume that the ergodic angular distribution is isotropic, the calculation of $C_1(t)$ becomes very simple, namely,

$$C_1(t) \;=\; \frac{1}{2}\left\langle \cos 2(\varphi_t - \varphi_0)\right\rangle \;=\; \frac{1}{2}\mathrm{e}^{-4D|t|} \qquad (23)$$

This expression implies a correlation time $\tau = 1/(2D)$, such that $c_1 = (1/2)\Delta_1\tau$ is half the "area" of the correlation function whose "height" is $\Delta_1 = 1/2$. Thus we get for the radial diffusion coefficient $D_r = w^2/(8D)$.

But in fact the ergodic angular distribution is not isotropic, meaning that X_1 is not zero, and $\Delta_1 < 1/2$. If w is not too large we may assume that the correlation time τ is not affected. Then it follows that a reasonable approximation for the correlation function is

$$C_1(t) \;\approx\; \Delta_1 \mathrm{e}^{-2|t|/\tau} \qquad (24)$$

leading to

$$D_r \;\approx\; \frac{1}{2}\Delta_1\tau w^2 \;=\; \Delta_1\frac{w^2}{4D} \qquad (25)$$

This approximation is compared to the exact result that we derive later in Fig.2. Unlike the rough approximation $D_r = w^2/(8D)$, it captures the observed non-monotonic dependence of D_r versus w, but quantitatively it is an over-estimate.

VI. THE EXACT CALCULATION OF THE DIFFUSION COEFFICIENT

We now turn to find an exact expression for the diffusion coefficient Eq.(22) by calculating c_1 of Eq.(17). Propagating an initial distribution $\rho_0(\varphi)$ with the FPE Eq.(12) we define the moments:

$$x_n \;=\; \left\langle \cos(2n\,\varphi_t)\right\rangle_0 \;=\; \left\langle \cos(2n\,\varphi)\right\rangle_t$$
$$=\; \int \cos(2n\,\varphi)\;\rho_t(\varphi)d\varphi \qquad (26)$$

The moments equation of motion resulting from the FPE is [10]:

$$\frac{d}{dt}x_n \;=\; -\Lambda_n\, x_n \;+\; W_n\,(x_{n-1} - x_{n+1}) \qquad (27)$$

where $\Lambda_n = 4Dn^2$ and $W_n = wn$. Due to $\Lambda_0 = W_0 = 0$ the zeroth moment $x_0 = 1$ does not change in time. Thus the rank of Eq.(27) is less than its dimension reflecting the existence of a zero mode $x_n = X_n$ that corresponds to the steady state of the FPE. We shall use the subscript "∞" to indicate the steady state distribution. Any other solution $x_n(t)$ goes to X_n in the long time limit, while all the other modes are decaying. To find X_n the equation should be solved with the boundary condition $X_\infty = 0$, and normalized such that $X_0 = 1$. Clearly this is not required in practice: because we already know the steady state solution Eq.(12), hence Eq.(15).

We define $x_n(t;\varphi_0)$ as the time-dependent solution for an initial preparation $\rho_0(\varphi) = \delta(\varphi - \varphi_0)$. Then we can express the correlation function of Eq.(16) as follows:

$$C_n(t) \;=\; \left\langle x_n(t;\varphi)\cos(2\varphi)\right\rangle_\infty - X_n X_1 \qquad (28)$$

By linearity the $C_n(t)$ obey the same equation of motion as that of the $x_n(t)$, but with the special initial conditions $C_n(0) = \Delta_n$. Note that $C_0(t) = 0$ at any time. In the infinite time limit $C_n(\infty) = 0$ for any n.

Our interest is in the area c_n as defined in Eq.(17). Writing Eq.(27) for $C_n(t)$, and integrating it over time we get

$$\Lambda_n\, c_n \;-\; W_n\,(c_{n-1} - c_{n+1}) \;=\; \Delta_n \qquad (29)$$

This equation should be solved with the boundary conditions $c_0 = 0$ and $c_\infty = 0$. The solution is unique because the $n = 0$ site has been effectively removed, and the truncated matrix is no longer with zero mode. One possible numerical procedure is to start iterating with c_1 as initial condition, and to adjust it such that the solution will go to zero at infinity. An optional procedure is to integrate the recursion backwards as explained in the next section. The bottom line is the following expression

$$D_r \;=\; c_1 w^2 \;=\; -\sum_{n=1}^{\infty}\frac{(-1)^n}{n}\Delta_n X_n w \qquad (30)$$

where X_n and Δ_n are given by Eq.(15) and Eq.(18) respectively.

The leading term approximation $D_r \approx \Delta_1 X_1 w$ is consistent with the heuristic expression $D_r \approx (1/2)\Delta_1 \tau w^2$ of Eq.(25) upon the identification

$$\tau \;=\; \frac{2}{w}\left[1-\exp\left(-\frac{w}{4D}\right)\right] \tag{31}$$

This expression reflects the crossover from diffusion-limited ($\tau \propto 1/D$) to drift-limited ($\tau \propto 1/w$) spreading. Fig. 2 compares the approximation that is based on Eq.(25) with Eq.(31) to the exact result Eq.(30).

In the limit $(w/D) \to 0$ the asymptotic result for the radial diffusion coefficient is $D_r = w^2/(8D)$. We now turn to figure out what is the asymptotic result in the other extreme limit $(w/D) \to \infty$. The large w/D approximation that is based on the first term of Eq. (30), with the limiting value $X_1 = 1$, provides the asymptotic estimate $D_r \approx 2D^2/w$. This expression is based on the asymptotic result Eq.(19) for Δ_n with $n = 1$. In fact we can do better and add all the higher order terms. Using Abel summation we get

$$D_r \;=\; 2\frac{D^2}{w}\sum_{n=1}^{\infty}(-1)^{n-1}n \;=\; \frac{1}{2}\frac{D^2}{w} \tag{32}$$

Thus the higher order terms merely add a factor 1/4 to the asymptotic result. If we used Eq.(25), we would have obtained the wrong prediction $D_r \approx D/2$ that ignores the τ dependence of Eq.(31).

VII. DERIVATION OF THE RECURSIVE SOLUTION

In this section we provide the details of the derivation that leads from Eq. (29) to Eq. (30). We define $W_n^{\pm} = \mp W_n$ and rewrite the equation in the more general form

$$-W_n^+ c_{n+1} + \Lambda_n c_n - W_n^- c_{n-1} \;=\; \Delta_n \tag{33}$$

A similar problem was solved in [11], while here we present a much simpler treatment. First we solve the associated homogeneous equation. The solution $c_n = X_n$ satisfies

$$-W_n^+ X_{n+1} + \Lambda_n X_n - W_n^- X_{n-1} \;=\; 0 \tag{34}$$

and one can define the ratios $R_n = X_n/X_{n-1}$. Note that these ratios satisfies a simple first-order recursive relation. However we bypass this stage because we can extract the solution from the steady state distribution.

We write the solution of the non-homogeneous equation as

$$c_n \;:=\; X_n \tilde{c}_n \tag{35}$$

and we get the equation

$$-W_n^+ X_{n+1}\tilde{c}_{n+1} + \Lambda_n X_n \tilde{c}_n - W_n^- X_{n-1}\tilde{c}_{n-1} \;=\; \Delta_n$$

Clearly it can be re-written as

$$-W_n^+ X_{n+1}(\tilde{c}_{n+1} - \tilde{c}_n) + W_n^- X_{n-1}(\tilde{c}_n - \tilde{c}_{n-1}) \;=\; \Delta_n$$

We define the discrete derivative

$$\tilde{a}_n \;:=\; \tilde{c}_n - \tilde{c}_{n-1} \tag{36}$$

And obtain a reduction to a first-order equation:

$$-W_n^+ X_{n+1}\tilde{a}_{n+1} + W_n^- X_{n-1}\tilde{a}_n \;=\; \Delta_n \tag{37}$$

This can be re-written in a simpler way by appropriate definition of scaled variables. Namely, we define the notations

$$\tilde{R}_n \;=\; \frac{W_n^+}{W_n^-}R_n \qquad\qquad \tilde{\Delta}_n \;=\; \frac{\Delta_n}{W_n^+} \tag{38}$$

and the rescaled variable

$$a_n \;:=\; X_n \tilde{a}_n \tag{39}$$

and then solve the a_n recursion in the backwards direction:

$$a_\infty = 0; \qquad a_n = \tilde{R}_n\left[\tilde{\Delta}_n + a_{n+1}\right] \tag{40}$$

If all the R_n were unity it would imply that $a_1 - a_\infty$ equals $\sum \Delta_n$. So it is important to verify that the "area" converges. Next we can solve in the forward direction the c_n recursion for the non-homogeneous equation, namely,

$$c_0 = 0; \qquad c_n = R_n c_{n-1} + a_n \tag{41}$$

In fact we are only interested in

$$c_1 \;=\; a_1 \;=\; \tilde{R}_1\tilde{\Delta}_1 + \tilde{R}_1\tilde{R}_2\tilde{\Delta}_2 + ... \tag{42}$$

Note that in our calculation the $\tilde{R}_n = -R_n$, and therefore $\tilde{R}_1 \cdots \tilde{R}_n = (-1)^n X_n$.

VIII. THE MOMENTS OF THE RADIAL SPREADING

The moments of a lognormal distribution are given by the following expression

$$\ln\langle r^n\rangle \;=\; \mu n \;+\; \frac{1}{2}\sigma^2 n^2 \tag{43}$$

On the basis of the discussion after Eq. (7), if one assumed that the radial spreading at time t could be *globally* approximated by the lognormal distribution (tails included), it would follow that

$$\frac{d}{dt}\ln\langle r^n\rangle \;=\; n w_r + n^2 D_r \tag{44}$$

In Fig.5 we plot the lognormal-based expected growth-rate of the 2nd and the 4th moments as a function of w/D. For small w/D there is a good agreement with the expected results, which are w^2/D and $3w^2/D$ respectively. For large w/D the dynamics is dominated by the stretching, meaning that $w_r \approx w$, while $D_r \to 0$, so again we have a trivial agreement. But for intermediate values of w/D the lognormal moments constitute an overestimate when compared with the exact analytical results

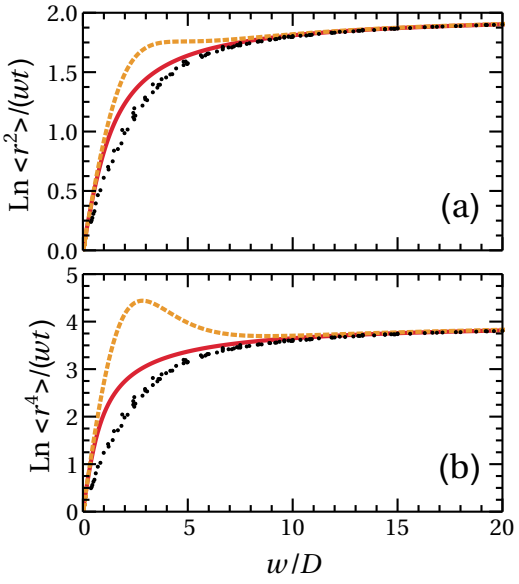

FIG. 5. Scaled moments versus w/D. The red solid lines are the exact results for the 2nd and 4th moments, given by Eq.(45) and Eq.(60), and the large w/D asymptotic values are at 2 and 4, respectively. These are compared with the numerical results (black symbols), and contrasted with the Lognormal prediction (orange dashed lines). The later provides an overestimate for intermediate values of w/D.

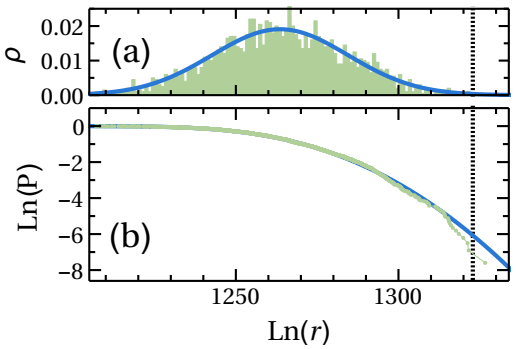

FIG. 6. **(a)** Distribution of $\ln(r)$ for $w/D = 10/3$ after time $wt = 2000$ with initial conditions $r = 1$ and $\varphi = 0$. Numerical results (green histogram), that are based on 2000 realizations, are fitted to a Gaussian distribution (blue line). **(b)** Inverse cumulative probability of the same distribution. The black dotted line indicate the numerically determined value $\ln\langle r^2\rangle^{1/2} \approx 1323$. This value is predominated by the tail of the distribution. The Gaussian fit fails to reproduce this value, and provides a gross over-estimate $\ln\langle r^2\rangle^{1/2} \approx 1701$.

that we derive in the next section. In fact also the exact analytical result looks like an overestimate when compared with the results of numerical simulations. But the latter is clearly a sampling issue that is explained in Appendix D.

The deviation of the lognormal moments from the exact results indicates that the statistics of large deviations is not captured by the central limit theorem. This point is illuminated in Fig.6. The Gaussian approximation constitutes a good approximation for the body of the distribution but not for the tails that dominate the moment-calculation. Clearly, the actual distribution can be described as a *bounded* lognormal distribution, meaning that it has a natural cutoff which is implied by the strict inequality $w_r < w$. The stretching rate cannot be faster than w. But in fact, as observed in Fig.6b, the deviation from the lognormal distribution happens even before the cutoff is reached.

Below we carry out an exact calculation for the 2nd and 4th moments. In the former case we show that

$$\frac{d}{dt}\ln\langle r^2\rangle \;\sim\; 2\left((w^2+D^2)^{1/2}-D\right) \qquad (45)$$

This agree with the lognormal-based prediction w^2/D for $(w/D) \ll 1$, and goes to $2w$ for $(w/D) \gg 1$, as could be anticipated.

Before we go the derivation of this result we would like to illuminates its main features by considering a simple-minded reasoning. Let us ask ourselves what would be the result if the spreading was isotropic ($w_r = 0$). In such case the moments of spreading can be calculated as if we are dealing with the multiplication of random numbers. Namely, assuming that the duration of each step is $\tau = 1/(2D)$, and treating t as a discrete index, Eq.(6) implies that the spreading is obtained by multiplication of uncorrelated stretching factors $\exp[w\tau\cos(\varphi)]$. Each stretching exponent has zero mean and dispersion $\sigma_1^2 = (1/2)[w\tau]^2$, which implies $D_r = \sigma_1^2/(2\tau)$. Consequently we get for the moments

$$\langle r^n\rangle \;=\; \left[\left\langle \mathrm{e}^{nw\tau\cos(2\varphi)}\right\rangle\right]^{t/\tau} r_0^n \qquad (46)$$

leading to

$$\frac{d}{dt}\ln\langle r^n\rangle \;=\; \frac{1}{\tau}\ln\left[I_0\left(\sqrt{2}n\sigma_1\right)\right] \qquad (47)$$

This gives a crossover from $n^2 D_r$ for $\sigma_1 \ll 1$ to nw for $\sigma_1 \gg 1$, reflecting isotropic lognormal spreading in the former case, and pure stretching in the latter case. So again we see that the asymptotic limits are easily understood, but for the derivation of the correct interpolation, say Eq.(45), further effort is required.

IX. THE EXACT CALCULATION OF THE MOMENTS

We turn to perform an exact calculation of the moments. The Langevin equation Eq.(1) is of the general form

$$\dot{x_j} \;=\; v_j + G_j\,\omega(t) \qquad (48)$$

$$\langle\omega(t)\omega(t')\rangle = 2D\delta(t-t') \qquad (49)$$

Namely, Eq. (1) is obtained upon the identification $x_j = (x, y)$ and $v_j = (x, -y)$, and $G_j = (-y, x)$. The

Stratonovich interpretation is used in order to associate with it an FPE, from which the Ito equation of motion for the moments can be derived, namely,

$$\frac{d}{dt}\langle X\rangle = \left\langle \frac{\partial X}{\partial x_j}\left(v_j + \frac{\partial G_j}{\partial x_i}DG_i\right)\right\rangle + \left\langle \frac{\partial^2 X}{\partial x_i \partial x_j}G_j DG_i\right\rangle \quad (50)$$

For the first moments we get

$$\langle \dot{x}\rangle = w\langle x\rangle - D\langle x\rangle \quad (51)$$
$$\langle \dot{y}\rangle = -w\langle y\rangle - D\langle y\rangle \quad (52)$$

with the solution

$$\langle x\rangle = x_0\,\exp[-(D-w)t] \quad (53)$$
$$\langle y\rangle = y_0\,\exp[-(D+w)t] \quad (54)$$

For the second moments

$$\frac{d}{dt}\begin{pmatrix}\langle x^2\rangle\\ \langle y^2\rangle\end{pmatrix} = \Big[-2D + 2D\boldsymbol{\sigma}_1 + 2w\boldsymbol{\sigma}_3\Big]\begin{pmatrix}\langle x^2\rangle\\ \langle y^2\rangle\end{pmatrix} \quad (55)$$

$$\frac{d}{dt}\langle xy\rangle = -4D\langle xy\rangle \quad (56)$$

where $\boldsymbol{\sigma}$ are Pauli matrices. The solution is:

$$\begin{pmatrix}\langle x^2\rangle\\ \langle y^2\rangle\\ \langle xy\rangle\end{pmatrix} = \begin{bmatrix} e^{-2Dt}\boldsymbol{M} & 0\\ 0 & e^{-4Dt}\end{bmatrix}\begin{pmatrix}x_0^2\\ y_0^2\\ x_0y_0\end{pmatrix} \quad (57)$$

where $\boldsymbol{M}$ is the following matrix:

$$\cosh[2(w^2+D^2)^{1/2}t] + \sinh[2(w^2+D^2)^{1/2}t]\frac{D\boldsymbol{\sigma}_1 + w\boldsymbol{\sigma}_3}{\sqrt{w^2+D^2}}$$

For an initial isotropic distribution we get $\langle r^2\rangle_t = Mr_0^2$, where

$$M = e^{-2Dt}\cosh[2(w^2+D^2)^{1/2}t] + \frac{D}{\sqrt{w^2+D^2}}e^{-2Dt}\sinh\left[2(w^2+D^2)^{1/2}t\right] \quad (58)$$

The short time t dependence is quadratic, reflecting "ballistic" spreading, while for long times

$$\langle r^2\rangle_t \approx \frac{r_0^2}{2}\left(1+\frac{D}{\sqrt{w^2+D^2}}\right)\times \exp\left[2\left((w^2+D^2)^{1/2}-D\right)t\right] \quad (59)$$

From here we get Eq.(45). For the 4th moments the equations are separated into two blocks of even-even powers and odd-odd powers in x and y. For the even block:

$$\frac{d}{dt}\begin{pmatrix}\langle x^4\rangle\\ \langle x^2y^2\rangle\\ \langle y^4\rangle\end{pmatrix} = 2\tilde{\boldsymbol{M}}\begin{pmatrix}\langle x^4\rangle\\ \langle x^2y^2\rangle\\ \langle y^4\rangle\end{pmatrix} \quad (60)$$

where

$$\tilde{\boldsymbol{M}} = \begin{pmatrix}2(w-D) & 6D & 0\\ D & -6D & D\\ 0 & 6D & -2(w+D)\end{pmatrix} \quad (61)$$

The eigenvalues of this matrix are the solution of $\lambda^3 + 10D\lambda^2 + (16D^2 - 4w^2)\lambda - 24Dw^2 = 0$. There are two negative roots, and one positive root. For small w/D the latter is $\lambda \approx (3/2)(w^2/D)$, and we get that the growth-rate is $3w^2/D$ as expected from the log-normal statistics.

X. DISCUSSION

In this work we have studied the statistics of a stochastic squeeze process, defined by Eq. (1). Consequently we are able to provide a quantitatively valid theory for the description of the noise-affected decoherence process in bimodal Bose-Einstein condensates, aka QZE. As the ratio w/D is increased, the radial diffusion coefficient of $\ln(r)$ changes in a non-monotonic way from $D_r = w^2/(8D)$ to $D_r = D^2/(2w)$, and the non-isotropy is enhanced, namely the average stretching rate increases from $w_r = w^2/(4D)$ to the bare value $w_r = w$. The analytical results Eq.(20) and Eq.(30) are illustrated in Fig.1 and Fig.2,

Additionally we have solved for the moments of r. One observes that the central limit theorem is not enough for this calculation, because the moments are predominated by the non-Gaussian tails of the $\ln(r)$ distribution. In particular we have derived for the second moment the expression $\langle r^2\rangle_t = Mr_0^2$ with M that is given by Eq.(58), or optionally one can use the practical approximation Eq.(45).

Let us clarify the experimental significance of the results that we have obtained for the full statistics of the radial spreading. In an actual experiment the standard approach is to perform a "fringe feasibility" measurement that corresponds, from a theoretical perspective, to the expectation value of some operator (it is essentially like measurement of an occupation difference). This leads to the definition of the coherence $\mathcal{F}(t)$ in terms of the Bloch vector. In our notations it is the expectation value of some operator $\hat{S} = S(\hat{x},\hat{y})$, see Appendix C. For sake of discussion, let us say that we are interested in $\langle \hat{x}^2\rangle$. In a semiclassical perspective (Wigner function picture) the phase-space coordinate x satisfies Eq. (1), where $\omega(t)$ arises from frequent interventions, or measurements, or noise that comes from the surrounding. Using a Feynman-Vernon perspective, each x outcome of the experiment can be regarded as the result of one realization of the stochastic process. The "coherence" is determined by the second moment of $\hat{x}$. But it is implied by our discussion of the *sampling problem* that it is impractical to determine this second moment from any realistic experiment (rare events are not properly accounted). The reliable experimental procedure would be to keep the *full* probability distribution of the measured x variable, and to extract the μ and the σ that characterize its log-normal statistics. For the latter we predict non-trivial dependence on w/D.

Appendix A: The squeeze operation

The squeeze operation is described by a real symplectic matrix that has unit determinant and trace $|a|>2$. Any such matrix can be expressed as follows:

$$\boldsymbol{U} \;=\; \begin{pmatrix} a & b \\ c & d \end{pmatrix} \;=\; \pm \mathrm{e}^{\alpha \boldsymbol{H}} \qquad [ad-cb=1] \quad \text{(A1)}$$

where $\mathbf{H}$ is a real traceless matrix that satisfies $\boldsymbol{H}^2=1$. Hence it can be expressed as a linear combination of the three Pauli matrices:

$$\boldsymbol{H} \;=\; n_1\boldsymbol{\sigma}_1 + in_2\boldsymbol{\sigma}_2 + n_3\boldsymbol{\sigma}_3 \quad \text{(A2)}$$

with $n_1^2-n_2^2+n_3^2=1$. Consequently

$$\boldsymbol{U} \;=\; \pm\left[\cosh(\alpha)\mathbf{1}+\sinh(\alpha)\boldsymbol{H}\right] \quad \text{(A3)}$$

We define the canonical form of the squeeze operation as

$$\boldsymbol{\Lambda} \;=\; \begin{pmatrix} \exp(\alpha) & 0 \\ 0 & \exp(-\alpha) \end{pmatrix} \quad \text{(A4)}$$

Then we can obtain any general squeeze operation via similarity transformation that involves re-scaling of the axes and rotation, and on top an optional reflection.

We can operate with $\boldsymbol{U}$ on an initial isotropic cloud that has radius $r_0=1$. Then we get a stretched cloud that has spread $\langle r^2\rangle = \mathcal{A}\, r_0^2$, where

$$\mathcal{A} \;\equiv\; \langle r^2\rangle\big|_{r_0=1} \;=\; \cosh(2\alpha) \quad \text{(A5)}$$

We also define the "spreading" as

$$\mathcal{S} \;=\; \mathcal{A}-1 \;=\; 2\sinh^2(\alpha) \quad \text{(A6)}$$

The notation α has no meaning for a *stochastic* squeeze process, while the notation $\mathcal{A}\equiv\langle r^2\rangle$ still can be used. In the latter case the average is over the initial conditions and also over realizations of $\omega(t)$, implying that in Eq.(A5) the $\cosh(2\alpha)$ should be averaged over α.

Appendix B: Numerical simulations

The analysis of a stochastic process can be based either on a direct Langevin type approach, or on a solution of the associated Fokker-Plank equation [12]. While for the analytic treatment we have preferred the latter, for the numerical simulations we have preferred the former. So what we are doing is a straightforward evolution using a discretized version of Eq.(1). Namely, we divide the time into small dt intervals ($dt \ll \tau$), and regard t as a discrete index. The evolution of a vector $\boldsymbol{r}_t=(x_t,y_t)$ during each interval is given by $\boldsymbol{r}_{t+dt}=\boldsymbol{U}_t\boldsymbol{r}_t$, where

$$\boldsymbol{U}_t \;=\; \begin{pmatrix} \cos\alpha_t & -\sin\alpha_t \\ \sin\alpha_t & \cos\alpha_t \end{pmatrix} \begin{pmatrix} e^{w\,dt} & 0 \\ 0 & e^{-w\,dt} \end{pmatrix} \quad \text{(B1)}$$

The uncorrelated random variables α_t have zero mean, and are taken from a box distribution of width $\sqrt{24D\,dt}$, such that their variance is $2D\,dt$. The evolution over time t is obtained by multiplication of t/dt matrices. The radial coordinate r is calculated under the assumption that the the preparation is (x_0=1, y_0=0. Accordingly, what we calculate for each realization is

$$r \;=\; \sqrt{U_{xx}^2+U_{yx}^2} \quad \text{(B2)}$$

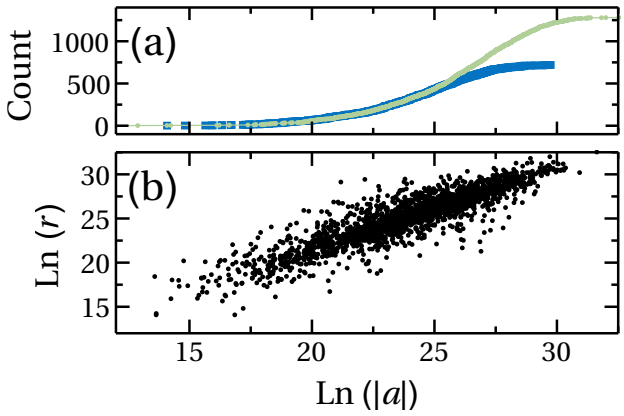

FIG. 7. We consider 2000 realizations of a stochastic squeeze process. For each realization the trace $a=\mathrm{trace}(\boldsymbol{U})$ is calculated. **(a)** The cumulative count of the a values. Green points are for positive values, while blue rectangles are for negative values. Here $(w/D)=10/3$ and $wt=40$. For simulations with longer times the distribution of positive and negative values become identical (not shown). **(b)** Scatter plot of $|a|$ versus the radial coordinate r. For simulations with longer times we get full correlation.

In Fig. 7a we display the distribution of the trace a for many realizations of such stochastic squeeze process. Rarely the result is a rotation, and therefore in the main text we refer to it as "squeeze". From the trace we get the squeeze exponent α, and from Eq. (B2) we get the radial coordinate r. The correlation between these two squeeze measures is illustrated in Fig. 7b. For the long time simulations that we perform in order to extract various moments, we observe full correlation (not shown). In order to extract the various moments, we perform the simulation for a maximum time of $wt=7500$, with the initial condition $\boldsymbol{r}_0=(1,0)$.

We note that the results of Section IX for the evolution of the moments can be recovered by averaging over product of the evolution matrices. For the first moments we get the linear relation $\langle \boldsymbol{r}_t\rangle = \langle \boldsymbol{U}\rangle\, \boldsymbol{r}_0$, where

$$\langle \boldsymbol{U}\rangle \;=\; \langle \ldots \boldsymbol{U}_{t_3}\,\boldsymbol{U}_{t_2}\,\boldsymbol{U}_{t_1}\rangle \;=\; [\langle \boldsymbol{U}_t\rangle]^{t/dt} = \begin{pmatrix} e^{-(D+w)t} & 0 \\ 0 & e^{-(D-w)t} \end{pmatrix} \quad \text{(B3)}$$

Similar procedure can be applied for the calculation of the higher moments.

Appendix C: Relation to QZE

It is common to represent the quantum state of the bosonic Josephson junction by a Wigner function on the Bloch sphere, see [1] for details. A coherent state is represented by a Gaussian-like distribution, namely

$$\rho^{(0)}(x,y) \approx 2\exp\left[-\frac{1}{\hbar}(x^2+y^2)\right] \tag{C1}$$

where x and y are local conjugate coordinates. The Wigner function is properly normalized with integration measure $dxdy/(2\pi\hbar)$. The dimensionless Plank constant is related to the number N of Bonsons, namely $\hbar=(N/2)^{-1}$. After a squeeze operation one obtains a new state $\rho^{(t)}(x,y)$. The survival probability is

$$\mathcal{P}(t)=\mathrm{Tr}\left[\rho^{(0)}\rho^{(t)}\right]=\frac{1}{\cosh(\alpha)}=\frac{1}{1+\frac{1}{2}\mathcal{S}(t)} \tag{C2}$$

However it is more common, both theoretically and experimentally to quantify the decay of the initial state via the length of the Bloch vector, namely $\mathcal{F}(t)=|\vec{S}(t)|$. It has been explained in [9] that

$$\mathcal{F}(t)\approx\exp\left\{-\hbar\sinh^2(\alpha)\right\}=\exp\left\{-\frac{\hbar}{2}\mathcal{S}(t)\right\} \tag{C3}$$

Comparing with the short time approximation of Eq. (C2), namely $\mathcal{P}\approx\exp[-(1/2)\mathcal{S}(t)]$, note the additional $\hbar=2/N$ factor in Eq. (C3). This should be expected: the survival probability drops to zero even if a single particle leaves the condensate. Contrary to that, the fringe visibility reflects the expectation value of the condensate occupation, and hence its decay is much slower. Still both depend on the spreading $\mathcal{S}(t)$.

The dynamics that is generated by Eq. (1) does not change the direction of the Bloch vector, but rather shortens its length, meaning that the one-body coherence is diminished, reflecting the decay of the initial preparation. Using the same coordinates as in [9] the Bloch vector is $\vec{S}(t)=(S,0,0)$, hence all the information is contained in the measurement of a single observable, aka fringe visibility measurement.

For a noiseless canonical squeeze operation we have $D=0$ and $\alpha=wt$, hence one obtains $\mathcal{S}(t)=2\sinh^2(wt)$ which is quadratic for short times. In contrast to that, for a stochastic squeeze process Eq.(C3) should be averaged over realizations of $\omega(t)$. Thus $\mathcal{F}(t)$ is determined by the full statistics that we have studied in this paper.

At this point we would like to remind the reader what is the common QZE argument that leads to the estimate of Eq. (4). One assumes that for strong D the time for phase randomization is $\tau=1/(2D)$. Dividing the evolution into τ-steps, and assuming that at the end of each step the phase is totally randomized (as in projective measurement) one obtains

$$\overline{\mathcal{A}(t)}\approx\left[\overline{\mathcal{A}(\tau)}\right]^{t/\tau}\approx\left[1-2(w\tau)^2\right]^{t/\tau} \tag{C4}$$

$$\approx\exp\left[(w^2/D)t\right] \tag{C5}$$

The overline indicates average over realizations, as discussed after Eq. (A5). The short time expansion of exponent is linear rather than quadratic, and the standard QZE expression Eq.(4) is recovered. This approximation is justified in the "Fermi Golden rule regime", namely for $\tau\ll t\ll t_r$, during which the deviation from isotropy can be treated as a first-order perturbation. For longer times, and definitely for weaker noise, the standard QZE approximation cannot be trusted.

Appendix D: Sample moments of a lognormal distribution

Consider a lognormal distribution of r values. This mean that the $\ln r$ values have a Gaussian distribution. For a finite sample of N values, one can calculate the sample average and the sample variance of the $\ln r$ values in order to get a *reliable* estimate for μ and σ, and then calculate the moments $\langle r^n\rangle$ via Eq.(43). But a direct calculation of these moments provides a gross underestimate as illustrated in Fig.8. This is because the direct average is predominated by rare values that belong to the tail of the distribution.

The lesson is that direct calculation of moments for log-wide distribution cannot be trusted. It can provide a lower bound to the true results, not an actual estimate.

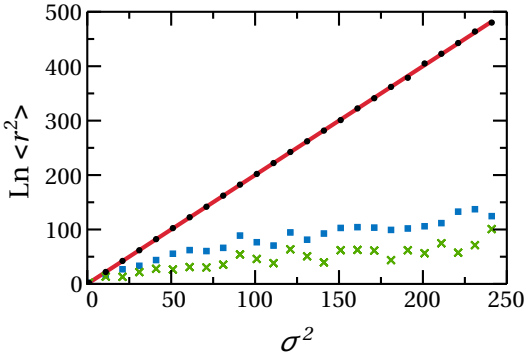

FIG. 8. $\ln\langle r^2\rangle$ versus σ for Lognormal distribution. Without loss of generality $\mu=0$. The true result is represented by red line. Numerical estimate based on 10^2 and 10^5 realizations are indicated by green crosses and blue rectangles, respectively. For the latter set of realization we get a much better estimate using an optional procedure (black dots). Namely, we calculate the sample average and the sample variance of the $\ln r$ values in order to determine μ and σ, and then use Eq.(43) to estimate the moments.

[1] M. Chuchem, K. Smith-Mannschott, M. Hiller, T. Kottos, A. Vardi, and D. Cohen, *Quantum dynamics in the bosonic Josephson junction*, Phys. Rev. A **82**, 053617 (2010).

[2] B. Misra and E. C. G. Sudarshan, *The Zeno's paradox in quantum theory*, Journal of Mathematical Physics **18**, 756 (1977).

[3] Wayne M. Itano, D. J. Heinzen, J. J. Bollinger, and D. J. Wineland, *Quantum Zeno effect*, Phys. Rev. A. **41**, 2295 (1990).

[4] M. C. Fischer, B. Gutirrez-Medina, and M. G. Raizen, *Observation of the Quantum Zeno and Anti-Zeno Effects in an Unstable System*, Phys. Rev. Lett. **87**, 040402 (2001)

[5] A. G. Kofman and G. Kurizki, *Universal Dynamical Control of Quantum Mechanical Decay: Modulation of the Coupling to the Continuum*, Phys. Rev. Lett. **87**, 270405 (2001).

[6] G. Gordon and G. Kurizki, *Preventing Multipartite Disentanglement by Local Modulations*, Phys. Rev. Lett. **97**, 110503 (2006).

[7] Y. Khodorkovsky, G. Kurizki, and A. Vardi, *Bosonic Amplification of Noise-Induced Suppression of Phase Diffusion*, Phys. Rev. Lett. **100**, 220403 (2008).

[8] Y. Khodorkovsky, G. Kurizki, and A. Vardi, *Decoherence and entanglement in a bosonic Josephson junction: Bose-enhanced quantum-Zeno control of phase-diffusion*, Phys. Rev. A **80**, 023609 (2009).

[9] C. Khripkov, A. Vardi, and D. Cohen, *Squeezing in driven bimodal Bose-Einstein condensates: Erratic driving versus noise*, Phys.Rev. A 85, 053632 (2012).

[10] H. Risken, *The Fokker-Planck Equation*, (Springer 1984).

[11] W. Coffey, Y. P. Kalmykov, and E. Massawe, *Effective-eigenvalue approach to the nonlinear Langevin equation for the Brownian motion in a tilted periodic potential. II. Application to the ring-laser gyroscope*, Phys. Rev. E 48, 699 (1993).

[12] P. Kloeden, E. Platenm, *Numerical Solution of Stochastic Differential Equations*, (Springer 1992).